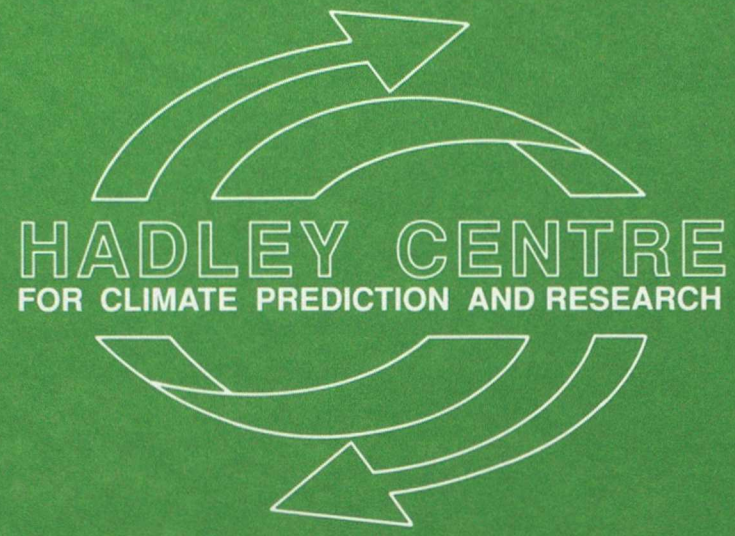

Causes and predictability of Sahel rainfall variability.

by

D. P. Rowell, C. K. Folland, K. Maskell,

J. A. Owen and M. N. Ward

CRTN 12 July 1991

CLIMATE
RESEARCH
TECHNICAL
NOTE

Hadley Centre
Meteorological Office
London Road
Bracknell
Berkshire RG12 2SY

CLIMATE RESEARCH TECHNICAL NOTE NO. 12

CAUSES AND PREDICTABILITY OF SAHEL RAINFALL VARIABILITY

by

D P ROWELL, C K FOLLAND, K MASKELL, J A OWEN and M N WARD

Hadley Centre for Climate Prediction and Research
Meteorological Office
London Road
Bracknell
Berkshire RG12 2SY
U.K.

Abstract

We describe a set of general circulation model experiments aimed at understanding the causes of interannual and interdecadal rainfall variability in the semi-arid Sahel region of North Africa, and the extent to which it might be predictable from sea surface temperature data. Ten individual years have been selected representing a broad cross-section of climate variability in the Sahel. When forced by observed global sea surface temperature data from the ten years, the model shows a considerable ability to simulate the observed seasonal (July to September) Sahel rainfall in all but one year. This provides strong support for the idea that oceanic effects tend to dominate the forcing of seasonal variability in the Sahel, though in some years moisture feedback from the land surface is also important. Interannual changes in the modelled atmospheric circulation are discussed, in particular moisture divergence and vertical motion over tropical North Africa, as well as the anomalous Walker-type circulations. From this we conclude that different atmospheric mechanisms may dominate in different years. Finally, experiments are presented which indicate that skilful predictions of July-September Sahel rainfall are possible using the persistence of June SST anomalies, but that skill deteriorates substantially when the lead time is increased by one or two months.

Introduction

The Sahel lies on the fringes of the Sahara close to the latitude of the northernmost limit of the inter-tropical convergence zone (ITCZ). The great majority of the rain falls between July and September, but amounts vary substantially on interannual and interdecadal time scales. The impact of drought on the livelihood and economy of the Sahelian people cannot be underestimated, so it is important that its causes and potential predictability be better understood.

Explanations of the variability of seasonal Sahel rainfall may be divided into two main categories: forcing from the ocean surface and forcing from the land surface [reviews by Druyan (1) and Nicholson (2)]. Some believe that the changing patterns of sea surface temperature (SST) dominate. A link with tropical Atlantic SSTs was first suggested by the empirical work of Lamb (3,4), and further studied by a number of other authors (5-9). More recent studies have shown that only when **global** SST patterns are considered can the variability of seasonal Sahel rainfall be best explained (10-15). Others contend that a feedback between land surface characteristics and the atmosphere may dominate, particularly on decadal and longer time scales [review by Nicholson (16)]. Three such mechanisms for the persistence of drought have been suggested: increased surface albedo due to the depletion of vegetation by anthropogenic or natural means (17-19); decreased availability of surface moisture (20,21); or enhanced concentrations of dust raised from a drier surface (22,23).

General circulation models provide an opportunity to test these ideas and to investigate possible mechanisms. This study follows the work of Folland et al. (10-12) and Palmer (13), but discusses a more extensive set of integrations.

The Model and Experimental Design

The general circulation model (GCM) used here has 11 levels in the vertical and a horizontal resolution of 2.5° latitude by 3.75° longitude. Physical parameterizations include: a diurnally and seasonally varying radiation scheme, interactive with water vapour, but with prescribed zonal mean cloud amounts; a mass-flux type convection scheme; boundary layer mixing in the lowest three layers; and a bucket type model of the surface hydrology where soil moisture content interacts with evaporation and precipitation (20,24).

For the first set of experiments the model was initiated from an atmospheric analysis for the 26 March 1984 and integrated through seven months to the end of October (denoted the GLOBAL84 set). The initial soil moisture distribution was taken from a 12-year model 'climatology' using a fixed annual cycle of SSTs. The impact of worldwide SST patterns on the variability of Sahel rainfall was tested by forcing the model with observed SST data from ten past years using the Meteorological Office Historical SST (MOHSST) data set (25). The ten years selected represent a broad cross-section of climate variability in the Sahel, including the dry year of 1949, the wet period of the 1950s (1950 and 1958), the long drought of the 1970s and 1980s (1976, 1983, 1984 and 1987), a return to near average rainfall in 1988 and 1989, and renewed drought in 1990. Monthly mean 5°x5° SST data were extended to cover data-sparse areas by blending observed data with a 1951-80 SST climatology (25) and 1951-80 climatological ice extents (26). Blending was done by adapting the Poisson equation technique originally used by Reynolds (27). Finally, the SST data were linearly interpolated to 5-day means on the model grid.

Each experiment was started at the end of March so as to allow two months for the model atmosphere to adjust to the imposed SSTs before the start of the Sahelian rainfall season. To test whether or not the

simulated Sahel rainfall was sensitive to the initial atmospheric conditions, the GLOBAL84 experiments were repeated, but with initial atmospheric data for 31 March 1987 and unchanged initial soil moisture content (denoted the GLOBAL87 set).

In a third set of experiments, the importance of intraseasonal variations in the availability of land surface moisture was tested by replacing the interactive soil moisture scheme with an evolving model derived soil moisture climatology (using initial data for 26 March 1984) (the CLIMSOIL set). Although we have not tested the sensitivity of the model to anomalies of the **initial** soil moisture distribution, any response to a realistic initial perturbation should be less than that of altering the land surface moisture feedback throughout the rainfall season.

The Sahel region used here consists of two rows of 14 grid points placed at 13.75°N and 16.25°N, and extending from 13.125°W to 35.625°E. The effective area sampled is thus 12.5°N to 17.5°N and 15°W to 37.5°E. This is similar to Nicholson's Sahel in the east, but in the west excludes some of its northern and extreme western parts, and to the south includes the northwestern part of her 'Soudan' region (28). Our aim is to investigate variability averaged over the entire Sahel region, but some of the analyses have been repeated for two sub-regions; 'West Sahel' and 'East Sahel'. Each comprise 2 x 7 grid points with the divide falling at 11.25°E. This is designed to assess the ability of the model to simulate interannual variations over different areas within the Sahel region, thus providing a more comprehensive analysis.

Fig.1 illustrates the quality of the model's spatial and temporal rainfall climatology. Observed gridded rainfall data for this paper were kindly provided by Dr M.Hulme of the Climatic Research Unit, Norwich. Fig.1a compares the model climatology calculated from the 20 GLOBAL84 and GLOBAL87 integrations with the observed 1956-85 climatology. The latter period was chosen as one with similar mean Sahel rainfall to that of the 10 selected years (a climatology directly comparable to the 10 modelled years is not shown because of insufficient data outside the Sahel). The observed climatology in Fig.1b was computed from the same 10 years as those simulated (grid boxes with missing data were filled in for each year by linear spatial interpolation of the anomalies). The model is seen to have a good regional rainfall climatology (apart from being too dry in the extreme western Sahel), demonstrating its suitability for studies of Sahel rainfall.

Influences of Sea Surface Temperature and Soil moisture feedback

Skill scores of the model's ability to simulate seasonal Sahel rainfall (July to September), when forced by SST data alone, is shown in Table 1 (first two rows). Its skill in individual years is illustrated in Figs.2a-c. Scores were calculated according to the definitions in Ward and Folland (29) [note that 'anomaly correlation' penalises bias, whereas standard correlation does not]. The model has high skill in all three regions, and sensitivity to the initial atmospheric data is relatively small. Noteworthy is the ability of the model to accurately simulate selected extreme years from the wet decade of the 1950s and the drought of the 1980s (1983, 1984 and 1987), adding weight to the idea that SST patterns are the main single cause of Sahel rainfall variability on decadal time scales. Fig.2 also demonstrates their importance in most individual years. The slight reduction in skill for the East and West Sahel compared to the whole Sahel arises from a small number of poor simulations in one or both sub-regions (Fig.2b,c), which is expected given their smaller size. The poorest simulation for the whole Sahel was for 1990, which incorrectly gave near average rainfall; in reality moderate or severe drought was experienced in all but the extreme west Sahel.

Table 1 and Fig.1d show the CLIMSOIL experiments to be almost as skilful as the GLOBAL84 and GLOBAL87 integrations, ie. **SST forcing appears to dominate the effects of land surface moisture feedback.**

However CLIMSOIL does have a lower standard deviation than GLOBAL84 and GLOBAL87 (0.92, 1.28 and 1.53 mm day^{-1}, respectively), suggesting a tendency for moisture feedback to increase the size of the rainfall anomalies (and also giving better ABSE scores for the former). Soil moisture feedback may also have played a significant secondary role in correctly determining the sign of the rainfall anomaly in 1976, and to a lesser extent in 1949.

When the temporal scale of analysis is reduced, from a season to a month, the correlation between the observed and modelled standardised monthly rainfall anomalies (for July, August and September) for the whole Sahel remains moderately high at 0.76 and 0.78 (GLOBAL84 and GLOBAL87 respectively). This suggests that the model also has skill in simulating the interannual variability of monthly rainfall. However, this variability comprises two components: first the interannual variability of seasonal rainfall (which has been shown to be well simulated), and second the monthly deviations from the seasonal mean (intraseasonal variability), which are calculated as:

$$I_{ij} = x_{ij} - \overline{x_j} \ , \quad where: \ \overline{x_j} = \tfrac{1}{3}\sum_{i=1}^{3} x_{ij}$$

and x_{1j}, x_{2j} and x_{3j} are standardised monthly rainfall anomalies for July, August and September in year j. For the whole Sahel, modelled and observed values of I are essentially uncorrelated for both GLOBAL84 (r=-0.20) and GLOBAL87 (r=-0.04). Possible explanations are: intraseasonal, monthly time-scale, variations may be dominated by non-oceanic effects (e.g. internal atmospheric variability); the model may be unable to correctly respond to SST variations on a monthly time scale; or that the deviations of monthly SSTs from their seasonal mean are inadequately measured. All three effects may be important.

Associated Atmospheric Circulation Changes

Some of the simulated changes in atmospheric circulation over tropical North Africa and their link to the distribution and variability of Sahel rainfall are now discussed. Only the time-mean (July to September) component of the flow is described as this dominates the eddy component. Seasonal means were compiled from six-hourly model data so as to adequately capture the mean effect of the diurnal cycle (20,30,31); this is important since both the modelled and observed diurnal cycles over tropical land regions are large. This was not done for GLOBAL87, so only GLOBAL84 diagnostics are shown.

Precipitation (P) over a specific region can be linked to the atmospheric circulation through the regional divergence of atmospheric moisture:

$$P = E - g^{-1}\int_{0}^{1} \nabla.\,(p_s q \mathbf{V})\ d\sigma - \Delta S$$

where E is evaporation, p_s is surface pressure, q is specific humidity, **V** is the 'horizontal' wind vector, $\sigma = p_s/p$ is the model's vertical coordinate system and ΔS is the change in regional atmospheric moisture storage. The importance of evaporation has already been discussed in the context of soil moisture feedback. The second term is the vertical integral of moisture divergence; the modelled 10-year mean vertical-latitudinal distribution of moisture divergence is illustrated in Fig.3a. This indicates that the Sahelian model atmosphere may be divided into three layers: below σ=0.9 (corresponding to about 850mb over the Sahel) there is rapid accumulation of moisture partly balanced by a divergence of moisture at mid-levels ($0.65<\sigma<0.9$), with negligible moisture accumulation/depletion at higher levels ($\sigma<0.65$). Figs. 3b and 3c illustrate the interannual variability of moisture divergence in each of the two lower layers and its

relationship to precipitation. It appears that locally two entirely different mechanisms of drought occur in the model: in 1984 and 1987 lack of precipitation is mainly linked to reduced **low-level** moisture convergence; but in 1983 it is increased **mid-level** divergence which is most important, and indeed moisture accumulation in the lowest two layers is actually largest in this year. The two simulated wet years are also primarily associated with changes in the mid-level divergence of moisture.

Other diagnostics not shown here reveal that the mid-level ($0.65<\sigma<0.9$) moisture divergence over the Sahel is strongly correlated with the latitude of the modelled 700mb African easterly jet ($r=-0.97$). In turn, the latitude of the jet is affected by rainfall over the Sahel ($r=0.91$) through changes to the meridional gradients of surface moisture and heating. This suggests a positive feedback cycle between moisture divergence, the jet, and rainfall; a relationship backed up by observational studies of the 700mb zonal flow and height field in wet and dry years (32,33).

We now separate moisture divergence (on σ surfaces) into two components:

$$p_s^{-1}\nabla.(p_s q V) = p_s^{-1} q \nabla.(p_s V) + V.\nabla q$$

(Each term has been scaled to units of $kgkg^{-1}s^{-1}$. The ∇p_s term within $\nabla.(p_s V)$ arises because of the sloping σ surfaces.) The first component on the right hand side is due to convergence of the flow, and the second is due to advection by the 'horizontal' flow. The divergent component is found to be much larger than the advective component (although the latter is by no means unimportant), and so the remaining paragraphs of this section concentrate only on the variability of the divergent flow and its link to rainfall. We also limit much of the discussion here to three of the more extreme years; 1950 (very wet), 1983 (very dry and related to strong divergence in the mid troposphere) and 1984 (very dry, but related to a weakening of low-level convergence).

Fig.4 shows examples of the simulated interannual variability of vertical motion. At all levels, the latitude of maximum modelled ascent is further north in 1950 than in the two drought years of 1983 and 1984, indicating that the ITCZ is similarly further north. Mid tropospheric ascent is also more intense in 1950 and penetrates to a greater depth, signifying a strengthening of the ITCZ. In the lowest layers however, at the latitude of the Sahel, upward motion is most intense in 1983. Above $\sigma=0.8$, the two dry years show increased mid level divergence (also Fig.3c) where the simulated Saharan subsidence has encroached further south than during the wet year. Observational studies of Sahel drought have disagreed as to whether changes in the latitude or intensity of the ITCZ are more important (3,4,6,33-35). Our sample of ten simulated years (including those not shown in Fig.4) seems to show that the latitude, intensity and slope of the ITCZ may all be important components of drought or wetness, whose relative importance varies from year to year.

Diagnostics of the variability of the zonal component of the divergent flow, or Walker-type circulations, may offer a way of identifying links between Sahel rainfall and atmospheric anomalies in distant regions. This is illustrated in Fig.5, which shows contours of the vertical integral of seasonal mean modelled zonal divergent mass flux. These can be interpreted as streamlines of the zonal divergent flow and its contribution to the vertical flow. Fig.5a shows the 10-year model climatology; this is consistent with the divergent circulation implied by analyses of velocity potential from observations in a 'normal' year (36). North Africa is influenced by the descending arms of large scale circulation cells centred on the Indian and Atlantic Oceans. The simulated anomalous response of the Walker-type circulations (Figs.5b-d and others not shown) is not always obviously related to the sign and magnitude of Sahel rainfall anomalies. 1984 for example shows only weak anomalous descent over North Africa (Fig.5d), despite being a year of severe drought,

indicating that other circulation features were more important. In 1950 and 1983 however changes in the Walker circulation are more closely linked to Sub-Saharan rainfall anomalies. In 1983 local anomalous descent from the Walker circulation was probably a major component of the severe modelled drought. Further study is needed to link this to the SST patterns, probably including the intense El Nino event in the tropical east Pacific.

Forecasting Experiments

The potential of the GCM for predicting seasonal (July to September) Sahel rainfall was tested for seven past years. Integrations again simulate the seven months from April to October, and start from 26 March 1984 initial data (except for the 1990 experiment, which as a real-time experimental forecast, started from 31 March 1990 data). However since the model was now being tested in forecast mode, the observed evolution of SSTs could not be assumed, and instead the SSTs had to be predicted. This was done by persisting the SST anomalies observed for either April, May or June through the remainder of the season and adding them to the seasonally evolving 1951-80 SST climatology. Fig.6 shows the resulting seven 'hindcasts' of seasonal rainfall. Consistently good results were obtained from June SST anomalies except for 1990, which (as already shown above) the model was unable to correctly simulate over the Sahel even from observed SSTs. As hindcast lead time increases, the skill decreases rapidly, so that anomaly correlations between modelled and observed rainfall drop from 0.87 (June) to 0.36 (May) and 0.28 (April).

Useful GCM forecasts from May or April will only become possible when better methods of (global) SST prediction are utilized than the crude technique of anomaly persistence adopted here. Some progress has already been made: for example regular experimental forecasts of El-Nino events are now published monthly in the Climate Diagnostics Bulletin (37) based on work by Cane et al. (38) and Barnett et al. (39). The need for such predictions is particularly well illustrated by the hindcasts for 1988, when an unusually large change in the pattern of SST anomalies occurred between April and June as a relatively strong El-Nino event decayed and a strong La-Nina event developed. The improvement in hindcast rainfall when using June 1988 instead of April 1988 SST anomalies is striking.

Conclusion

We believe the results presented here considerably strengthen the idea that variations in global and regional SST patterns have been the primary factor influencing the variability of seasonal Sahel rainfall on both interannual and interdecadal time scales through the twentieth century. Empirical studies indicate that much of the interdecadal variability, and a small part of the interannual component, may be linked to changes in an interhemispheric contrast of SST anomalies (10,40). A substantial part of the interannual signal is correlated with SSTs in the tropical Atlantic near Africa (12,14) and with El Nino (41,42). In some years the SST forcing is such that other factors in the model, such as soil moisture feedbacks, also play a key role. The simulations also indicate that the local atmospheric mechanisms of drought or wetness may differ substantially from year to year. A promising way to examine the links between the SST patterns and these atmospheric mechanisms is to carry out integrations forced by observed SSTs in one or more ocean basins only, with climatological SSTs elsewhere. About 50 such experiments are currently being analysed.

The potential of GCMs for skilful prediction of seasonal Sahel rainfall has also been analysed for a small sample of years. Skilful GCM forecasts seem possible only at the start of the peak of the rainfall season, unless SST variations can be reliably predicted a season in advance. Even then occasional failures are likely.

References

1. L.M.Druyan, Int. J. Climatol., 9, 77 (1989).
2. S.E.Nicholson, Am. Geophys. Union, Geophys. Monogr. 52, IUGG Vol.7, 79 (1989).
3. P.J.Lamb, Mon. Wea. Rev., 106, 482 (1978).
4. P.J.Lamb, Tellus, 30, 240 (1978).
5. S.Hastenrath, Mon. Wea. Rev., 112, 1097 (1984).
6. S.Hastenrath, Int. J. Climatol., 10, 459 (1990).
7. J.M.Lough, Mon. Wea. Rev., 114, 561 (1986).
8. P.J.Lamb, and R.A.Peppler, in "ENSO Teleconnections Linking Worldwide Climate Anomalies: Scientific Basis and Societal Impact", M.H. Glantz, R.W. Katz, N. Nicholls, Eds, (Cambridge University Press, 1991).
9. L.M.Druyan, Clim. Change, 18, 17 (1991).
10. C.K.Folland, T.N.Palmer, D.E.Parker, Nature, 320, 602 (1986).
11. C.K.Folland, J.A.Owen, K.Maskell, IAHS Publ. no. 186, 87 (1989).
12. C.K.Folland, J.A.Owen, M.N.Ward, A.Colman, J. Forecasting, 10, 21 (1991).
13. T.N.Palmer, Nature, 322, 251 (1986).
14. F.H.M.Semazzi, V.Mehta, Y.C.Sud, Atmos.-Ocean, 26, 118 (1988).
15. K.Wolter, J. Climate, 2, 149 (1989).
16. S.E.Nicholson, Progr. Phys. Geogr., 12, 36 (1988).
17. J.G.Charney, Q.J.R. Meteorol. Soc., 101, 193 (1975).
18. J.G.Charney, W.J.Quirk, S.H.Chow, J.Kornfield, J. Atmos. Sci., 34, 1366 (1977).
19. K.Laval, and L.Picon, J. Atmos. Sci., 43, 2418 (1986).
20. W.M.Cunnington, and P.R.Rowntree, Q.J.R. Meteorol. Soc., 112, 971 (1986).
21. Y.C.Sud, and A.Molod, Mon. Wea. Rev., 116, 2388 (1988).
22. J.M.Prospero, and R.T.Nees, Science, 196, 1196 (1977).
23. J.M.Prospero, and R.T.Nees, Nature, 320, 735 (1986).
24. A.Slingo, Ed., Dyn. Climatol. Tech. Note No. 29 (Met. Office, Bracknell, U.K., 1985)
25. M.Bottomley, C.K.Folland, J.Hsiung, R.E.Newell, D.E.Parker, Global ocean surface temperature atlas. Joint Met. Office/MIT Project. Funded by U.K. Depts. of Environment and Energy. 313 plates (HMSO, London, 1990).
26. R.C.Alexander, and R.L.Mobley, Mon. Wea. Rev., 104, 143 (1976).
27. R.W.Reynolds, J. Climate, 1, 75 (1988).
28. S.E.Nicholson, Mon. Wea. Rev., 108, 473 (1980).
29. M.N.Ward, and C.K.Folland, Int. J. Climatol., in press.
30. D.P.Rowell, Clim. Res. Tech. Note No.3 (Met. Office, Bracknell, U.K., 1990)
31. J.Thuburn, Q.J.R. Meteorol. Soc., 117, 385 (1991).
32. R.E.Newell, and J.W.Kidson, J. Climatol., 4, 27 (1984).
33. M.Shinoda, J. Meteor. Soc. Japan, 68, 613 (1990).
34. S.E.Nicholson, J. Clim. Appl. Meteorol., 25, 1365 (1986).
35. M.Debois, T.Kayiranga, B.Gnamien, S.Guessous, L.Picon, J. Climate, 1, 867 (1988).
36. M.Kanamitsu, and T.N.Krishnamurti, Mon. Wea. Rev., 106, 331 (1978).
37. Forecast Forum, in Climate Diagnostics Bulletin (issued monthly by Climate Analysis Center,Washington DC).
38. M.A.Cane, S.E.Zebiak, and S.C.Dolan, Nature, 321, 827 (1986).
39. T.Barnett, et al., Science, 241, 192 (1988).

40. D.E.Parker, C.K.Folland, M.N.Ward, in "Recent Climatic Change - a regional approach", S.Gregory, Ed. (Belhaven Press, London, 1988), chap. 15.
41. C.F.Ropelewski, and M.S.Halpert, Mon. Wea. Rev., 115, 1606 (1987).
42. C.F.Ropelewski, and M.S.Halpert, J. Climate, 2, 268 (1989).

Table 1 Skill scores of each experiment set for the Whole Sahel, West Sahel and East Sahel. ABSE is mean absolute error, and CHANCE ABSE is the ABSE expected by chance.

EXPERIMENT SET	ANOMALY CORRELATION			BIAS ($mm\ day^{-1}$)			ABSE ($mm\ day^{-1}$)			ABSE/CHANCE ABSE (%)		
	Whole	West	East	Whole	West	East	Whole	West	East	Whole	West	East
GLOBAL84	0.90	0.87	0.86	0.07	-0.22	0.36	0.47	0.71	0.42	37	44	43
GLOBAL87	0.94	0.94	0.87	0.29	0.13	0.45	0.45	0.74	0.48	32	41	43
CLIMSOIL	0.88	0.89	0.87	0.15	0.15	0.14	0.36	0.54	0.31	33	40	34

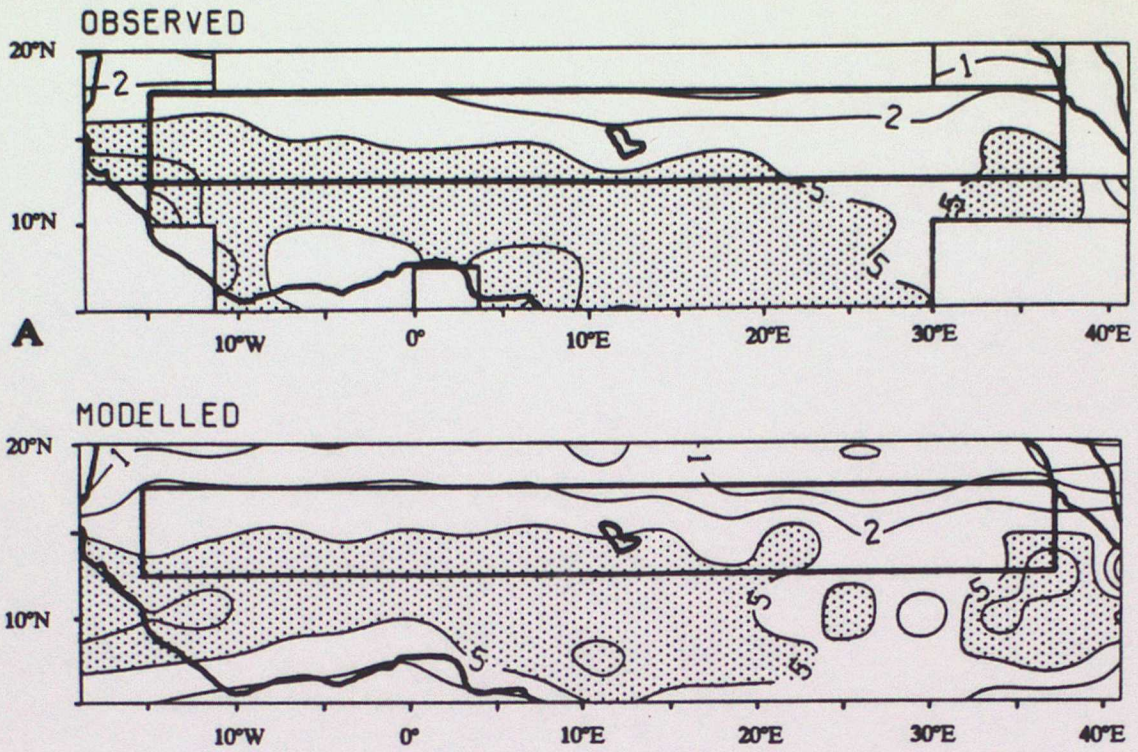

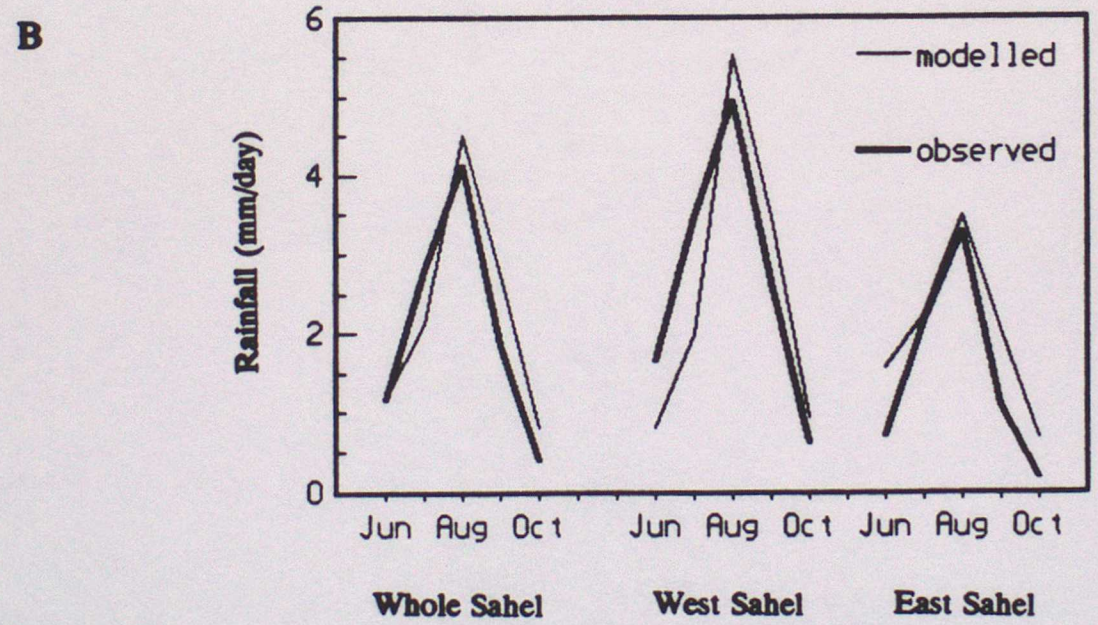

Fig.1 (a) Maps of July to Sept. climatological rainfall: 'observed' is 1956-85 average, and 'modelled' is based on the 10 years 1949, 1950, 1958, 1976, 1983, 1984, 1987, 1988, 1989, 1990. Thick boxed area marks the Sahel. Thin boxed areas (in the observed) have insufficient data to estimate mean rainfall. Contours: 1, 2, 5, 10, 15, 20 mm day^{-1}.

(b) Monthly observed and modelled rainfall (means of the 10 above years) averaged over the whole Sahel (12.5°N to 17.5°N, 15°W to 37.5°E), West Sahel (same latitudes, 15°W to 11.25°E) and East Sahel (11.25°E to 37.5°E).

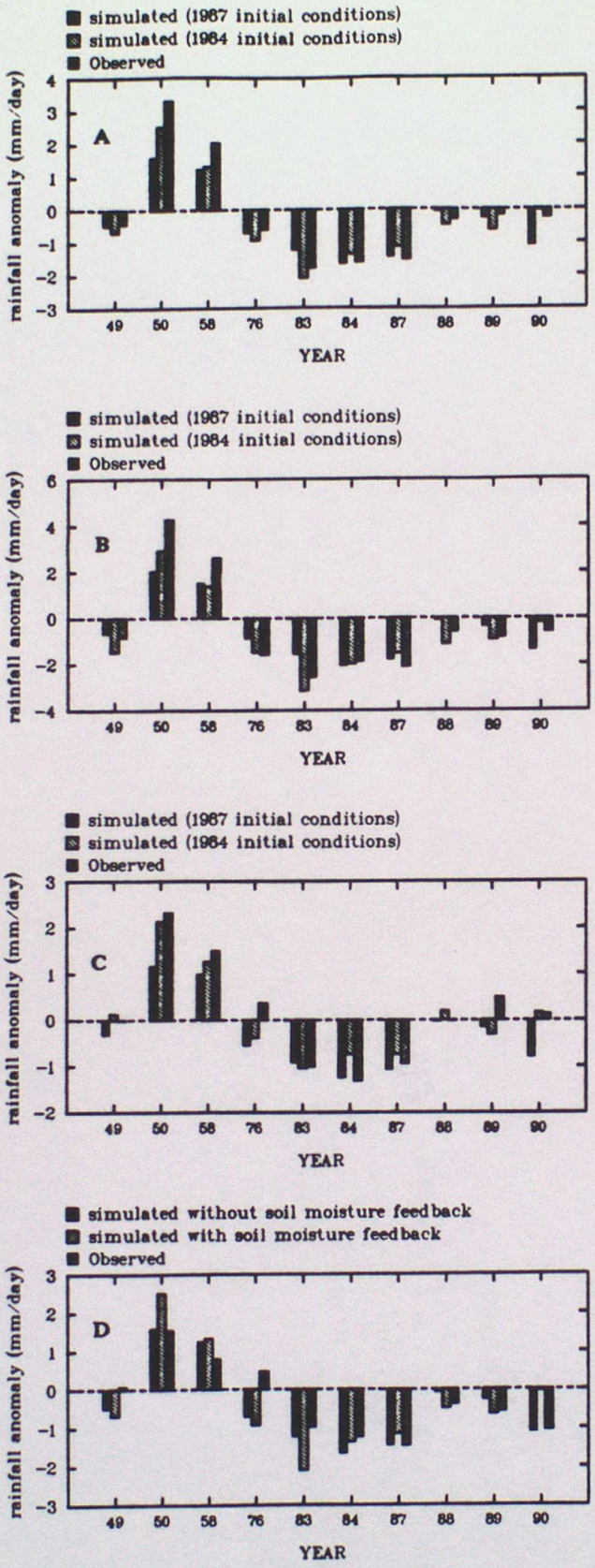

Fig.2 Histograms comparing simulated and observed July to Sept. rainfall anomalies for ten past years. GLOBAL84 and GLOBAL87 rainfall for (a) the whole Sahel, (b) West Sahel and (c) East Sahel. (d) CLIMSOIL and GLOBAL84 rainfall for the whole Sahel. The zero line is the observed 1951-80 climatology (3.36, 4.24, 2.48 and 3.36 mm day^{-1}, respectively).

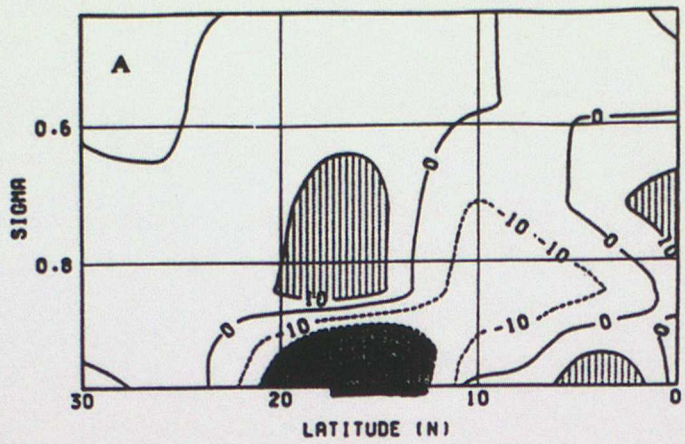

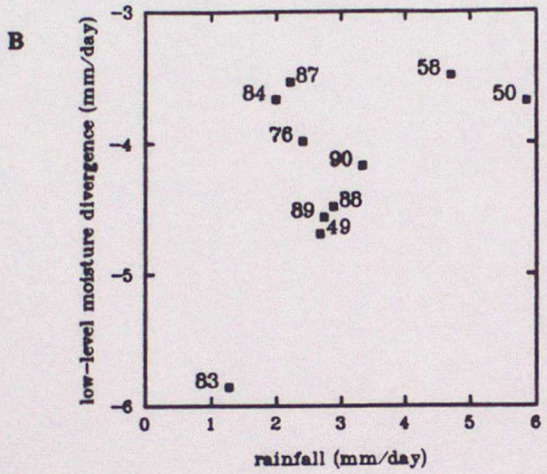

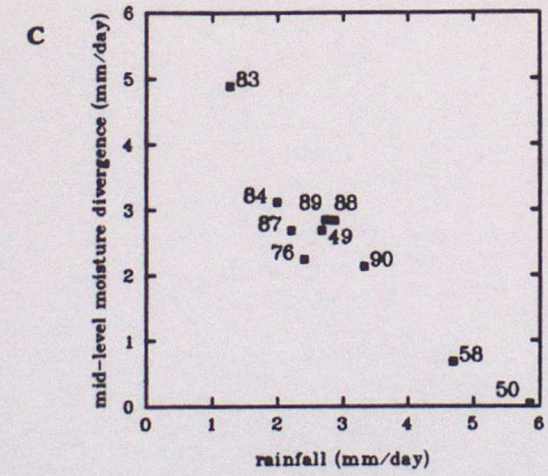

Fig.3 (a) Cross-section of July to Sept. moisture divergence ($p_s^{-1}\nabla.(p_s q V)$), averaged from 15°W to 37.5°E and meaned over the 10 GLOBAL84 simulations. Units: $kgkg^{-1}s^{-1} \times 10^9$. Solid rectangle indicates the Sahel region.

(b) Scatter diagram of July to Sept. moisture divergence in the two lowest model layers ($g^{-1}\int_{0.9}^{1} \nabla.(p_s q V)\, d\sigma$) averaged over the Sahel, against Sahel rainfall, for the 10 GLOBAL84 simulations. (c), as (b), but third and fourth model layers ($0.65<\sigma<0.9$).

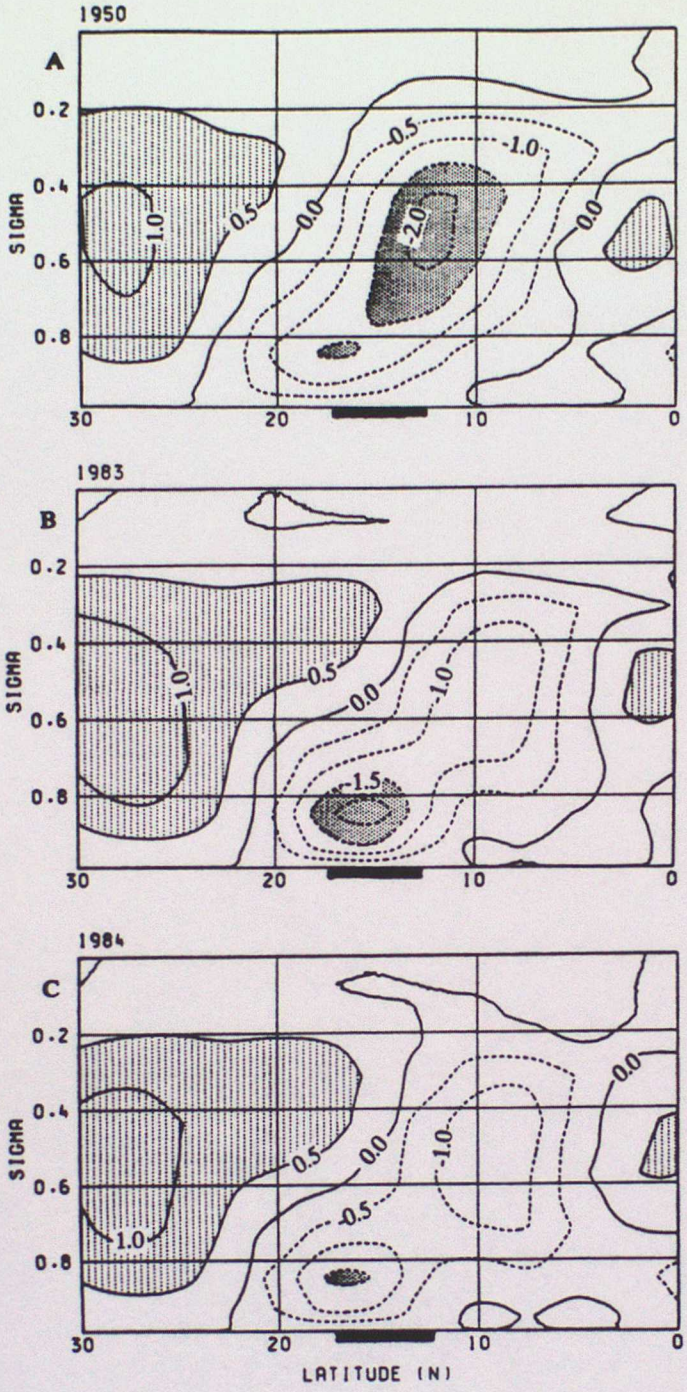

Fig.4 Cross-sections of July to Sept. vertical motion (dp_s/dt), averaged from 15°W to 37.5°E, for the (a) 1950, (b) 1983 and (c) 1984 GLOBAL84 simulations. Units: mb hr^{-1}. Solid rectangle indicates the Sahel.

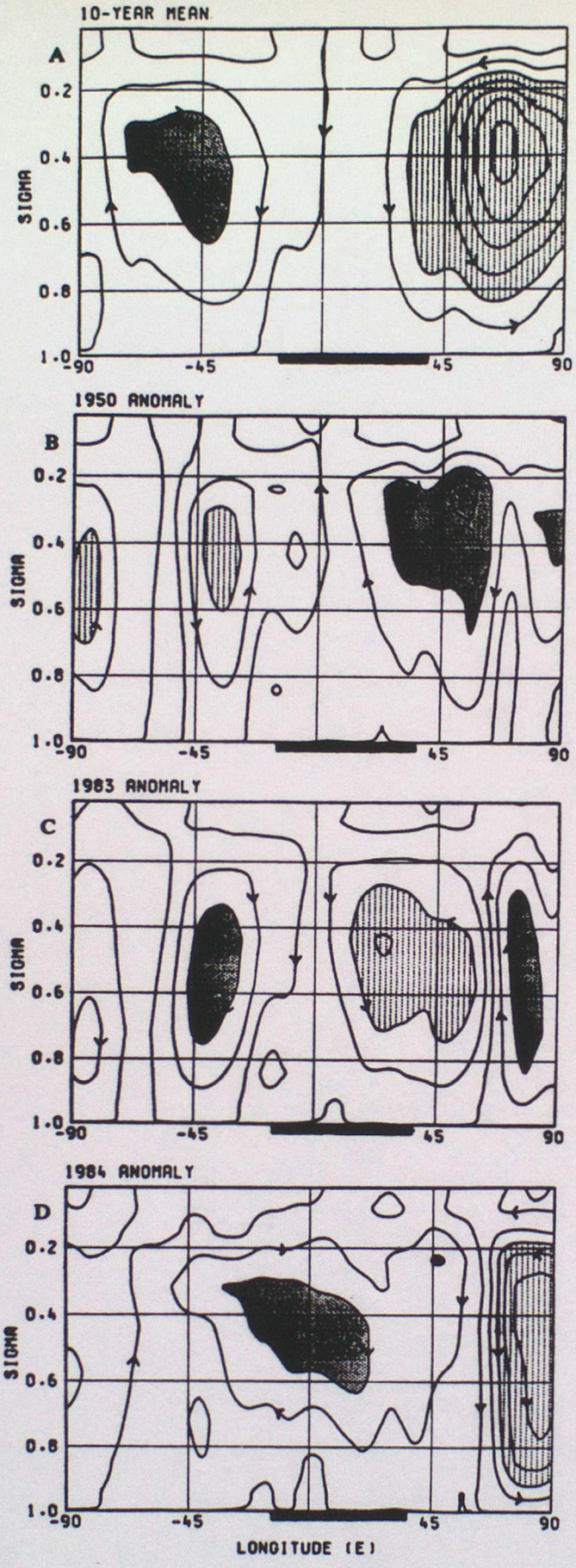

Fig.5 Cross-sections of the July to Sept. vertical integral of the zonal divergent component of mass flux averaged from 6°N to 24°N ($-\frac{a}{g}\int_{\pi/30}^{4\pi/30}\int_{1}^{o} p_s u_\chi \, d\sigma d\theta$, where a is the earth's radius, u_χ is zonal divergent wind and θ is latitude). Plotted for (a) the mean of the ten GLOBAL84 simulations; (b)-(d) anomalies from this mean for the (b) 1950, (c) 1983 and (d) 1984 simulations. Contour interval is $10^9 kgs^{-1}$ ($3x10^9 kgs^{-1}$ in (a)). Stippling is: light: > $2x10^9$; dense: < $-2x10^9$ ($\pm 6x10^9$ in (a)). Solid rectangle indicates the Sahel.

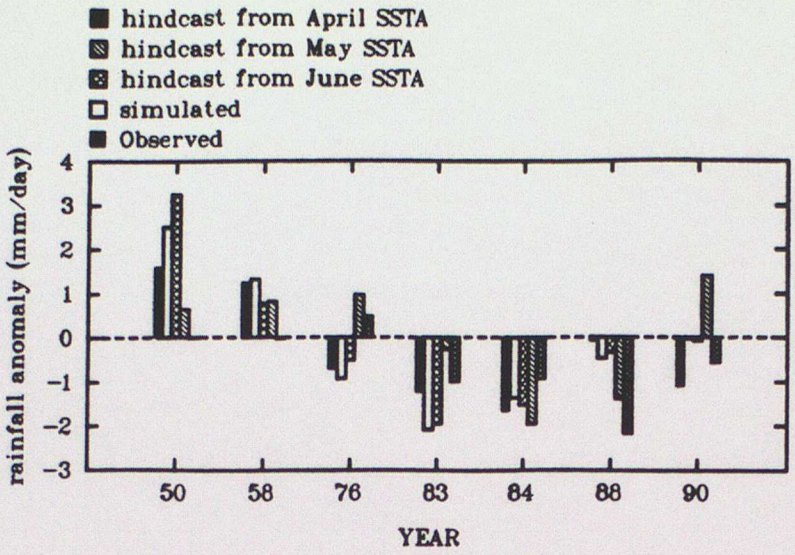

Fig.6 Histogram of the observed, simulated (GLOBAL84) and hindcast July to Sept. Sahel rainfall anomalies for 7 past years, including real-time experimental forecasts for 1990. The zero line is the observed 1951-80 climatology (3.36 mm day^{-1}).

CLIMATE RESEARCH TECHNICAL NOTES

CRTN 1	Oct 1990	Estimates of the sensitivity of climate to vegetation changes using the Penman-Monteith equation. P R Rowntree
CRTN 2	Oct 1990	An ocean general circulation model of the Indian Ocean for hindcasting studies. D J Carrington
CRTN 3	Oct 1990	Simulation of the tropical diurnal cycle in a climate model. D P Rowell
CRTN 4	Oct 1990	Low frequency variability of the oceans. C K Folland, A Colman, D E Parker and A Bevan
CRTN 5	Dec 1990	A comparison of 11-level General Circulation Model Simulations with observations in the East Sahel. K Maskell
CRTN 6	Dec 1990	Climate Change Prediction. J F B Mitchell and Qing-cun Zeng
CRTN 7	Jan 1991	Deforestation of Amazonia - modelling the effects of albedo change. M F Mylne and P R Rowntree
CRTN 8	Jan 1991	The role of observations in climate prediction and research. D J Carson
CRTN 9	Mar 1991	The greenhouse effect and its likely consequences for climate change. D J Carson
CRTN 10	Apr 1991	Use of wind stresses from operational N.W.P. models to force an O.G.C.M. of the Indian Ocean. D J Carrington
CRTN 11	Jun 1991	A new daily Central England Temperature series, 1772-1991. D E Parker, T P Legg and C K Folland
CRTN 12	Jul 1991	Causes and predictability of Sahel rainfall variability. D P Rowell, C K Folland, K Maskell, J A Owen, M N Ward